



CHORUS

This is the accepted manuscript made available via CHORUS. The article has been published as:

Electron-impact ionization of W^{27+}

M. S. Pindzola and S. D. Loch

Phys. Rev. A **93**, 062709 — Published 29 June 2016

DOI: [10.1103/PhysRevA.93.062709](https://doi.org/10.1103/PhysRevA.93.062709)

Electron-Impact Ionization of W^{27+}

M. S. Pindzola and S. D. Loch

Department of Physics, Auburn University, Auburn, AL, USA

(Received:)

Abstract

Electron-impact ionization cross sections for W^{27+} are calculated using a semi-relativistic configuration-average distorted-wave (CADW) method. Calculations for direct ionization, excitation-autoionization, and branching ratios are compared with recent calculations by Jonauskas et al. (PRA 91, 012715 (2015)) who used fully-relativistic subconfiguration-average distorted-wave (SCADW) and level to level distorted-wave (LLDW) methods. Reasonable agreement is found between the new CADW and the recent LLDW calculations for direct ionization of the $4l(l = 0 - 1, 3)$ subshells, but not the $4d$ subshell, and between the new CADW and recent SCADW/LLDW calculations for excitation-autoionization of the $4l(l = 0 - 2)$ subshells. Reasonable agreement is also found between the new CADW and the recent SCADW calculations including branching ratios, but both differ from the recent LLDW calculations. Additional CADW calculations are made for excitation-autoionization including branching ratios involving the important $3l(l = 1 - 2)$ subshells, not examined by Jonauskas et al. (PRA 91, 012715 (2015)).

I. INTRODUCTION

The use of an ITER full tungsten divertor [1] is being tested at a number of controlled fusion tokamaks, including JET [2] and ASDEX-UPGRADE [3]. The DIII-D tokamak is also performing experiments using tungsten [4]. Electron-ionization and electron-recombination rate coefficients are needed in impurity transport codes to predict the amount of tungsten present in the core of the controlled fusion tokamaks [5].

Several years ago electron-impact ionization cross sections were calculated for all atomic ions in the W isonuclear sequence [6]. The semi-relativistic configuration-average distorted-wave (CADW) method [7] was found to be very useful for calculating electron-impact ionization cross sections involving direct ionization, excitation-autoionization, and branching ratios. For example, the CADW total ionization cross sections were found to be in reasonable agreement with crossed-beams experimental measurements [8] for W^{4+} to W^{9+} . The CADW total ionization cross sections were found to be in reasonable agreement for W^{45+} with calculations made using a semi-relativistic level to level distorted-wave (LLDW) method [9], where branching ratios make large reductions in the excitation-autoionization contributions. For W^{64+} and more highly charged ions, the CADW direct ionization cross sections were found to grow larger in magnitude than more accurate results obtained using a fully-relativistic subconfiguration-average distorted-wave (SCADW) method [10,11].

Recently electron-impact ionization cross sections were calculated for W^{27+} using fully-relativistic sub-configuration average distorted-wave (SCADW) and level to level distorted-wave (LLDW) methods [12]. In this article we make new CADW calculations to check against the recent SCADW/LLDW calculations for direct ionization, excitation-autoionization, and branching ratios. The new CADW and recent LLDW calculations are found to be in reasonable agreement for direct ionization of the $4l(l = 0 - 1, 3)$ subshells, but not for the $4d$ subshell. Once the CADW calculations are extended to high nl , the need for being pointed out by Jonauskas et al. [12] for moderately to highly charged W atomic ions, the new CADW and recent SCADW/LLDW calculations for excitation autoionization

of the $4l(l = 0 - 2)$ subshells are found to be in reasonable agreement. Additional CADW calculations are made for excitation autoionization of the important $3l(l = 1 - 2)$ subshells, not considered in the recent SCADW/LLDW work [12]. Finally, the new CADW calculations including branching ratios of the $4l(l = 0 - 2)$ subshells are found to be in reasonable agreement with recent SCADW calculations, but not the recent LLDW calculations.

The rest of this paper is organized as follows. In Section II we give a brief review of the theoretical method used to calculate ionization cross sections. In Section III we present cross sections for W^{27+} . We conclude with a brief summary and future plans in Section IV. Unless otherwise stated, we will use atomic units.

II. THEORY

For direct ionization a general transition between configurations has the form:

$$(n_0 l_0)^{w_0} k_i l_i \rightarrow (n_0 l_0)^{w_0-1} k_e l_e k_f l_f , \quad (1)$$

where w_0 is a subshell occupation number, $n_0 l_0$ are quantum numbers of the bound electron, and $k_i l_i$, $k_e l_e$, and $k_f l_f$ are quantum numbers of the initial, ejected, and final continuum electrons. The configuration-average ionization cross section is given by [7]:

$$\begin{aligned} \sigma_{dir} = & \frac{32w_0}{k_i^3} \int_0^{E/2} \frac{d(k_e^2/2)}{k_e k_f} \\ & \times \sum_{l_i, l_e, l_f} (2l_i + 1)(2l_e + 1)(2l_f + 1) \mathcal{S}(n_0 l_0 k_i l_i \rightarrow k_e l_e k_f l_f) , \end{aligned} \quad (2)$$

where $E = \frac{k_e^2}{2} + \frac{k_f^2}{2}$ and $\mathcal{S}(n_0 l_0 k_i l_i \rightarrow k_e l_e k_f l_f)$ are partial scattering probabilities for ionization given in terms of 3j/6j symbols and radial Slater integrals [7].

For excitation a general transition between configurations has the form:

$$(n_1 l_1)^{w_1+1} (n_2 l_2)^{w_2-1} k_i l_i \rightarrow (n_1 l_1)^{w_1} (n_2 l_2)^{w_2} k_f l_f , \quad (3)$$

where w_1 and w_2 are subshell occupation numbers, $n_1 l_1$ and $n_2 l_2$ are quantum numbers of the bound electrons, and $k_i l_i$ and $k_f l_f$ are quantum numbers of the initial and final continuum electrons. The configuration-average excitation cross section is given by [7]:

$$\begin{aligned} \sigma_{exc} = & \frac{8\pi}{k_i^3 k_f} (w_1 + 1)(4l_2 + 3 - w_2) \\ & \times \sum_{l_i, l_f} (2l_i + 1)(2l_f + 1) \mathcal{S}(n_1 l_1 k_i l_i \rightarrow n_2 l_2 k_f l_f) , \end{aligned} \quad (4)$$

where $\mathcal{S}(n_1 l_1 k_i l_i \rightarrow n_2 l_2 k_f l_f)$ are partial scattering probabilities for excitation given in terms of 3j/6j symbols and radial Slater integrals [7].

For autoionization a general transition between configurations may have the form:

$$(n_1 l_1)^{w_1} (n_2 l_2)^{w_2} (n_3 l_3)^{w_3} \rightarrow (n_1 l_1)^{w_1+1} (n_2 l_2)^{w_2-1} (n_3 l_3)^{w_3-1} k_e l_e , \quad (5)$$

where w_1 , w_2 , and w_3 are subshell occupation numbers, $n_1 l_1$, $n_2 l_2$, and $n_3 l_3$ are quantum numbers of the bound electrons, and $k_e l_e$ are quantum numbers of the final continuum electron. The configuration-average autoionization rate is given by [7]:

$$\begin{aligned} A_{auto} = & \frac{(4l_1 + 2 - w_1) w_2 w_3}{k_e} \\ & \times (4l_e + 2) \mathcal{S}(n_2 l_2 n_3 l_3 \rightarrow n_1 l_1 k_e l_e) . \end{aligned} \quad (6)$$

For autoionization a general transition between configurations may also have the form:

$$(n_1 l_1)^{w_1} (n_2 l_2)^{w_2} \rightarrow (n_1 l_1)^{w_1+1} (n_2 l_2)^{w_2-2} k_e l_e \quad (7)$$

and the configuration-average autoionization rate is given by [7]:

$$\begin{aligned} A_{auto} = & \frac{(4l_1 + 2 - w_1) w_2 (w_2 - 1) (4l_2 + 2)}{k_e (4l_2 + 1)} \\ & \times (4l_e + 2) \mathcal{S}(n_2 l_2 n_2 l_2 \rightarrow n_1 l_1 k_e l_e) . \end{aligned} \quad (8)$$

where $\mathcal{S}(n_2 l_2 n_3 l_3 \rightarrow n_1 l_1 k_e l_e)$ and $\mathcal{S}(n_2 l_2 n_2 l_2 \rightarrow n_1 l_1 k_e l_e)$ are autoionization probabilities given in terms of 3j/6j symbols and radial Slater integrals [7].

For radiative decay a general transition between configurations has the form:

$$(n_1 l_1)^{w_1-1} (n_2 l_2)^{w_2} \rightarrow (n_1 l_1)^{w_1} (n_2 l_2)^{w_2-1} , \quad (9)$$

where w_1 and w_2 are subshell occupation numbers and $n_1 l_1$ and $n_2 l_2$ are quantum numbers of the bound electrons. The configuration-average radiative rate is given by [7]:

$$A_{rad} = \frac{8\omega^3 (4l_1 + 3 - w_1)w_2}{3c^3 (4l_1 + 2)(4l_1 + 2)} \times l_{>} \mathcal{S}(n_2l_2 \rightarrow n_1l_1), \quad (10)$$

where ω is the transition frequency, c is the speed of light, $l_{>} = \max(l_1, l_2)$, and $\mathcal{S}(n_2l_2 \rightarrow n_1l_1)$ are radiative probabilities given in terms of radial dipole matrix elements [7].

The bound radial orbitals needed for the calculations of the scattering probabilities are obtained by using a Hartree-Fock semi-relativistic (HFR) atomic structure code [13]. The continuum radial orbitals needed for the calculations of the scattering probabilities are obtained by solving the radial Schrodinger equation.

III. RESULTS

To show the pathways available for ionization, excitation, and autoionization, we present the energy level diagram in Figure 1. The ionization potentials for the outer subshells of W^{27+} are found in Table I and are labeled $nl - ion$ in Figure 1. The ionization potential for the $4d$ subshell of W^{28+} for $3s^23p^63d^{10}4s^24p^64d^{10} \rightarrow 3s^23p^63d^{10}4s^24p^64d^9$ is 1136.7 eV. The excitation energies to the $4f$ subshell for the outer subshells of W^{27+} are found in Table II and are labeled $nl \rightarrow 4f$ in Figure 1. The vertical arrows indicate the range of energies for the $4d, 4p, 4s, 3d, 3p, 3s \rightarrow nl$ excitations.

A. Direct Ionization

Based on Figure 1, the direct ionization contribution to the single ionization of W^{27+} includes the first four transitions found in Table I involving the $4f, 4d, 4p,$ and $4s$ subshells. The final three transitions involving the $3d, 3p,$ and $3s$ subshells contribute to the multiple ionization of W^{27+} . The CADW results based on calculations using Eq.(2) are presented in Figure 2 for the direct ionization of the $4l$ ($l = 0 - 3$) subshells. The peak of the total direct ionization cross section is near 2690 eV and has a value of 0.27 Mb. The differences between the direct ionization cross sections shown in the CADW results of Figure 2 and the

LLDW results of Figure 6 of Jonauskas et al. [12] is attributed to differences in the CADW and LLDW results for the $4d$ subshell.

B. Excitation-Autoionization

Based on Figure 1, the excitation-autoionization contribution to the single ionization of W^{27+} involves the $4d$, $4p$, $4s$, $3d$, and $3p$ subshells. For single ionization the excitations must have energies that exceed the $4f$ ionization potential of 878.4 eV. Double ionization is likely to occur for excitations whose energies exceed the $3d$ ionization potential of 2782.8 eV.

Involving the $4d$ subshell, we considered 110 excitations beginning with the $4d \rightarrow 4f$ at 211.2 eV and extending to the $4d \rightarrow 20i$ at 1060.7 eV. Only 89 excitations are found to be above the $4f$ ionization potential, the first being the $4d \rightarrow 8d$ at 886.1 eV. Involving the $4p$ subshell, we considered 75 excitations beginning with the $4p \rightarrow 4f$ at 423.8 eV and extending to the $4p \rightarrow 15i$ at 1253.5 eV. Only 67 excitations are found to be above the $4f$ ionization potential, the first being the $4p \rightarrow 6p$ at 915.5 eV. Involving the $4s$ subshell, we considered 40 excitations beginning with the $4s \rightarrow 4f$ at 584.6 eV and extending to the $4s \rightarrow 10i$ at 1356.0 eV. Only 36 excitations are found to be above the $4f$ ionization potential, the first being the $4s \rightarrow 5f$ at 953.6 eV. Selected threshold cross sections for the $4l(l = 0 - 2)$ subshells are given in Table III.

Involving the $3d$ subshell, we considered 40 excitations beginning with the $3d \rightarrow 4f$ at 1895.2 eV and extending to the $3d \rightarrow 10i$ at 2676.0 eV. All 40 excitations are found to be above the $4f$ ionization potential. Involving the $3p$ subshell, we considered 6 excitations beginning with the $3p \rightarrow 4f$ at 2438.1 eV and extending to the $3p \rightarrow 5g$ at 2882.1 eV. Only 4 excitations are found to be above the $4f$ ionization potential and below the $3d$ ionization potential, the first being the $3p \rightarrow 4f$ and the last being the $3p \rightarrow 5d$ at 2727.8 eV. We note that all excitations involving the $3s$ subshell are above the $3d$ ionization potential and are most likely to contribute to double ionization. Selected threshold cross sections for the $3l(l = 1 - 2)$ subshells are given in Table III.

The CADW results based on the calculations using Eq.(4) are presented in Figure 3 for the excitation-autoionization of the $4l(l = 0 - 2)$ and $3l(l = 1 - 2)$ subshells. The SCADW results from Figure 5 of Jonauskas et al. [12] are also shown in Figure 3. The largest contribution is at 1895.2 eV and involves the transition $3d \rightarrow 4f$. Reasonable agreement is found between the CADW results of Figure 3 for the excitation of the $4l(l = 0 - 2)$ subshells below the $3d \rightarrow 4f$ excitation at 1895.2 eV and the SCADW and LLDW results of Figure 5 of Jonauskas et al. [12]. Thus we confirm that excitation to high nl subshells is required for the moderately charged W^{27+} atomic ion. We note that SCADW and LLDW calculations were not carried out for the $3l(l = 1 - 2)$ subshells.

C. Branching Ratios

Based on Figure 1, branching ratios need to be calculated for all 236 excitations that lie between the $4f$ and $3d$ ionization potentials.

The $4d \rightarrow nl$ excitations include the possibility of $4f \rightarrow 4d$ autoionization and $4f \rightarrow 4d$ radiative decay. The $4p \rightarrow nl$ excitations include the possibility of $4d \rightarrow 4p$ and $4f \rightarrow 4p$ autoionization and $4d \rightarrow 4p$ radiative decay. The $4s \rightarrow nl$ excitations include the possibility of $4f \rightarrow 4s$, $4d \rightarrow 4s$, and $4p \rightarrow 4s$ autoionization and $4p \rightarrow 4s$ radiative decay.

The $3d \rightarrow nl$ excitations include the possibility of $4f \rightarrow 3d$, $4d \rightarrow 3d$, $4p \rightarrow 3d$, and $4s \rightarrow 3d$ autoionization and $4f \rightarrow 3d$ and $4p \rightarrow 3d$ radiative decay. Finally, the $3p \rightarrow nl$ excitations include the possibility of $4f \rightarrow 3p$, $4d \rightarrow 3p$, $4p \rightarrow 3p$, $4s \rightarrow 3p$, and $3d \rightarrow 3p$ autoionization and $4d \rightarrow 3p$, $4s \rightarrow 3p$, and $3d \rightarrow 3p$ radiative decay.

In general, the strongest autoionization rate involves the transfer of an electron from the closest subshell, as shown in Table IV for the decay of the $3s^2 3p^6 3d^{10} 4s 4p^6 4d^{10} 4f 10s$ configuration. Selected excitation cross sections and branching ratios for the $4l(l = 0 - 2)$ and $3l(l = 1 - 2)$ subshells are given in Table V.

The CADW results based on the calculations using Eqs.(4), (6), (8), and (10) are presented in Figure 3 for the excitation of the $4l(l = 0 - 2)$ and $3l(l = 1 - 2)$ subshells including

branching ratios. The SCADW results with branching ratios from Figure 5 of Jonauskas et al. [12] are also shown in Figure 3. Reasonable agreement is found between the CADW results of Figure 3 for the excitation of the $4l(l = 0 - 2)$ subshells below the $3d \rightarrow 4f$ excitation at 1895.2 eV and the SCADW results of Figure 5 of Jonauskas et al. [12]. However, differences are found between the CADW and SCADW results and the LLDW results.

Using a semi-relativistic level to level distorted-wave method [14], we performed branching ratio calculations for the $3d \rightarrow 4f$, $3d \rightarrow 5s$, and $3d \rightarrow 5p$ excitations. We find that our CADW and averaged LLDW results agree to within a couple of percent for these W^{27+} transitions.

D. Total Ionization

The total ionization cross section for the single ionization of W^{27+} is presented in Figure 4. Direct ionization includes contributions from the $4l(l = 0 - 3)$ subshells of the $3s^2 3p^6 3d^{10} 4s^2 4p^6 4d^{10} 4f$ ground configuration made using the CADW method. Excitation-autoionization includes contributions from 236 excitations of the $4l(l = 0 - 2)$ and $3l(l = 1 - 2)$ subshells and their respective branching ratios made using the CADW method. The peak of the total ionization cross section is near 2449 eV and has a value of 0.50 Mb.

IV. SUMMARY

Electron-impact ionization cross sections for W^{27+} were calculated using a semi-relativistic CADW method. Reasonable agreement was found between the new CADW calculations and recent LLDW calculations [12] for direct ionization involving the $4l(l = 0 - 1, 3)$ subshells, but not for the $4d$ subshell. Reasonable agreement was found between the new CADW calculations and the recent SCADW/LLDW calculations [12] for excitation-autoionization involving the $4l(l = 0 - 2)$ subshells. CADW calculations were also made for excitation-autoionization involving the important $3l(l = 1 - 2)$ subshells. The largest single excitation-autoionization contribution involves the $3d \rightarrow 4f$ excitation. Reasonable

agreement was also found between the new CADW calculations and the recent SCADW calculations [12] including branching ratios involving the $4l(l = 0 - 2)$ subshells. CADW calculations were also made including branching ratios involving the important $3l(l = 1 - 2)$ subshells.

In the future, we plan to make calculations using the semi-relativistic LLDW method [9] for the excitation-autoionization cross sections and branching ratios for the $4d \rightarrow 8l(l = 2 - 6)$, $4p \rightarrow 6l(l = 2 - 5)$, and $4s \rightarrow 5l(l = 3 - 4)$ transitions to check against our CADW results and the LLDW results of Jonauskas et al. [12]. Hopefully we will find reasonable agreement between the semi-relativistic CADW and LLDW calculations, since the use of the LLDW method for complicated moderately charged W atomic ions is quite a computational challenge.

ACKNOWLEDGMENTS

This work was supported in part by grants from the US Department of Energy and the US National Science Foundation. Computational work was carried out at the National Energy Research Scientific Computing Center in Oakland, California.

REFERENCES

- [1] S Carpentier-Chouchana et al., Phys. Scr. T **159**, 014002 (2014)
- [2] G F Matthews et al., Physica Scripta T **167**, 014070 (2016)
- [3] U Stroth et al., Nuclear Fusion **53**, 104003 (2013).
- [4] D L Rudakov et al., Physica Scripta T **167**, 014055 (2016)
- [5] T Putterich, R Nea, R Dux, A D Whiteford, M G O'Mullane, H P Summers, and the ASDEX-UPGRADE Team, Nuclear Fusion **50**, 025012 (2010)
- [6] S D Loch, J A Ludlow, M S Pindzola, A D Whiteford, and D C Griffin, Phys. Rev. A **72**, 052716 (2005)
- [7] M S Pindzola, D C Griffin, and C Bottcher, NATO ASI B **145**, 75 (1986)
- [8] M Stenke, K Aichele, D Hathiramani, G Hofmann, M Steidl, R Volpel, and E Salzborn, J. Phys. B **28**, 2711 (1995)
- [9] D C Griffin, C Bottcher, and M S Pindzola, Phys. Rev. A **25**, 1374 (1982).
- [10] M S Pindzola and M J Buie, Phys. Rev. A **37**, 3232 (1988).
- [11] M S Pindzola, D L Moores, and D C Griffin, Phys. Rev. A **40**, 4941 (1989).
- [12] V Jonauskas, A Kyniene, G Merkelis, G Giagalus, R Kisielius, S Kucas, S Masys, L Radziute, and P Rynkun, Phys. Rev. A **91**, 012715 (2015)
- [13] R D Cowan, *The Theory of Atomic Structure and Spectra* (1981)
- [14] N R Badnell, J. Phys. B **19**, 3827 (1986)

TABLES

TABLE I. Ionization potentials for W^{27+}

Initial Configuration	Final Configuration	Ionization potential
$3s^23p^63d^{10}4s^24p^64d^{10}4f$	$3s^23p^63d^{10}4s^24p^64d^{10}$	878.4 eV
	$3s^23p^63d^{10}4s^24p^64d^94f$	1087.4 eV
	$3s^23p^63d^{10}4s^24p^54d^{10}4f$	1300.9 eV
	$3s^23p^63d^{10}4s4p^64d^{10}4f$	1462.8 eV
	$3s^23p^63d^94s^24p^64d^{10}4f$	2782.8 eV
	$3s^23p^53d^{10}4s^24p^64d^{10}4f$	3325.7 eV
	$3s3p^63d^{10}4s^24p^64d^{10}4f$	3775.7 eV

TABLE II. Excitation energies for W^{27+}

Initial Configuration	Final Configuration	Excitation energy
$3s^23p^63d^{10}4s^24p^64d^{10}4f$	$3s^23p^63d^{10}4s^24p^64d^94f^2$	211.2 eV
	$3s^23p^63d^{10}4s^24p^54d^{10}4f^2$	423.8 eV
	$3s^23p^63d^{10}4s4p^64d^{10}4f^2$	584.6 eV
	$3s^23p^63d^94s^24p^64d^{10}4f^2$	1895.2 eV
	$3s^23p^53d^{10}4s^24p^64d^{10}4f^2$	2438.1 eV
	$3s3p^63d^{10}4s^24p^64d^{10}4f^2$	2887.9 eV

TABLE III. Selected threshold excitation cross sections for W^{27+} ($1.0 \text{ kb} = 1.0 \times 10^{-21} \text{ cm}^2$)

Transition	Angular Momenta	Cross Section
$4d \rightarrow 8l$	2-6	68.1 kb
$4d \rightarrow 9l$	0-6	45.6 kb
$4d \rightarrow 10l$	0-6	30.5 kb
$4d \rightarrow 15l$	0-6	7.6 kb
$4d \rightarrow 20l$	0-6	3.0 kb
$4p \rightarrow 6l$	2-5	46.2 kb
$4p \rightarrow 7l$	0-6	38.6 kb
$4p \rightarrow 10l$	0-6	9.0 kb
$4p \rightarrow 15l$	0-6	2.2 kb
$4s \rightarrow 5l$	3-4	12.6 kb
$4s \rightarrow 6l$	0-5	18.1 kb
$4s \rightarrow 10l$	0-6	1.9 kb
$3d \rightarrow 4l$	3	72.3 kb
$3d \rightarrow 5l$	0-4	28.0 kb
$3d \rightarrow 10l$	0-6	2.0 kb
$3p \rightarrow 4l$	3	10.9 kb
$3p \rightarrow 5l$	0-2	3.9 kb

TABLE IV. Autoionization rates for W^{27+}

Initial Configuration	Final Configuration	Autoionization rate
$3s^2 3p^6 3d^{10} 4s 4p^6 4d^{10} 4f 10s$	$3s^2 3p^6 3d^{10} 4s^2 4p^5 4d^{10} 4f$	$9.5 \times 10^{13} \text{ Hz}$
	$3s^2 3p^6 3d^{10} 4s^2 4p^6 4d^9 4f$	$2.0 \times 10^{13} \text{ Hz}$
	$3s^2 3p^6 3d^{10} 4s^2 4p^6 4d^{10}$	$8.6 \times 10^{11} \text{ Hz}$

TABLE V. Selected excitation cross sections and branching ratios for W^{27+} (1.0 kb = 1.0×10^{-21} cm²)

Transition	Cross Section	Branching Ratio
$4d \rightarrow 8d$	21.0 kb	0.99
$4d \rightarrow 8f$	11.9 kb	0.96
$4d \rightarrow 8g$	24.1 kb	0.99
$4d \rightarrow 8h$	9.7 kb	0.99
$4d \rightarrow 8i$	1.4 kb	0.97
$4p \rightarrow 6d$	8.8 kb	0.55
$4p \rightarrow 6f$	11.8 kb	0.60
$4p \rightarrow 6g$	21.8 kb	0.64
$4p \rightarrow 6h$	3.9 kb	0.46
$4s \rightarrow 5f$	4.7 kb	0.72
$4s \rightarrow 5g$	7.9 kb	0.76
$3d \rightarrow 4f$	72.3 kb	0.96
$3d \rightarrow 5s$	0.6 kb	0.71
$3d \rightarrow 5p$	1.3 kb	0.71
$3d \rightarrow 5d$	8.5 kb	0.84
$3d \rightarrow 5f$	16.8 kb	0.78
$3d \rightarrow 5g$	1.0 kb	0.26
$3p \rightarrow 4f$	10.9 kb	0.68

FIGURES

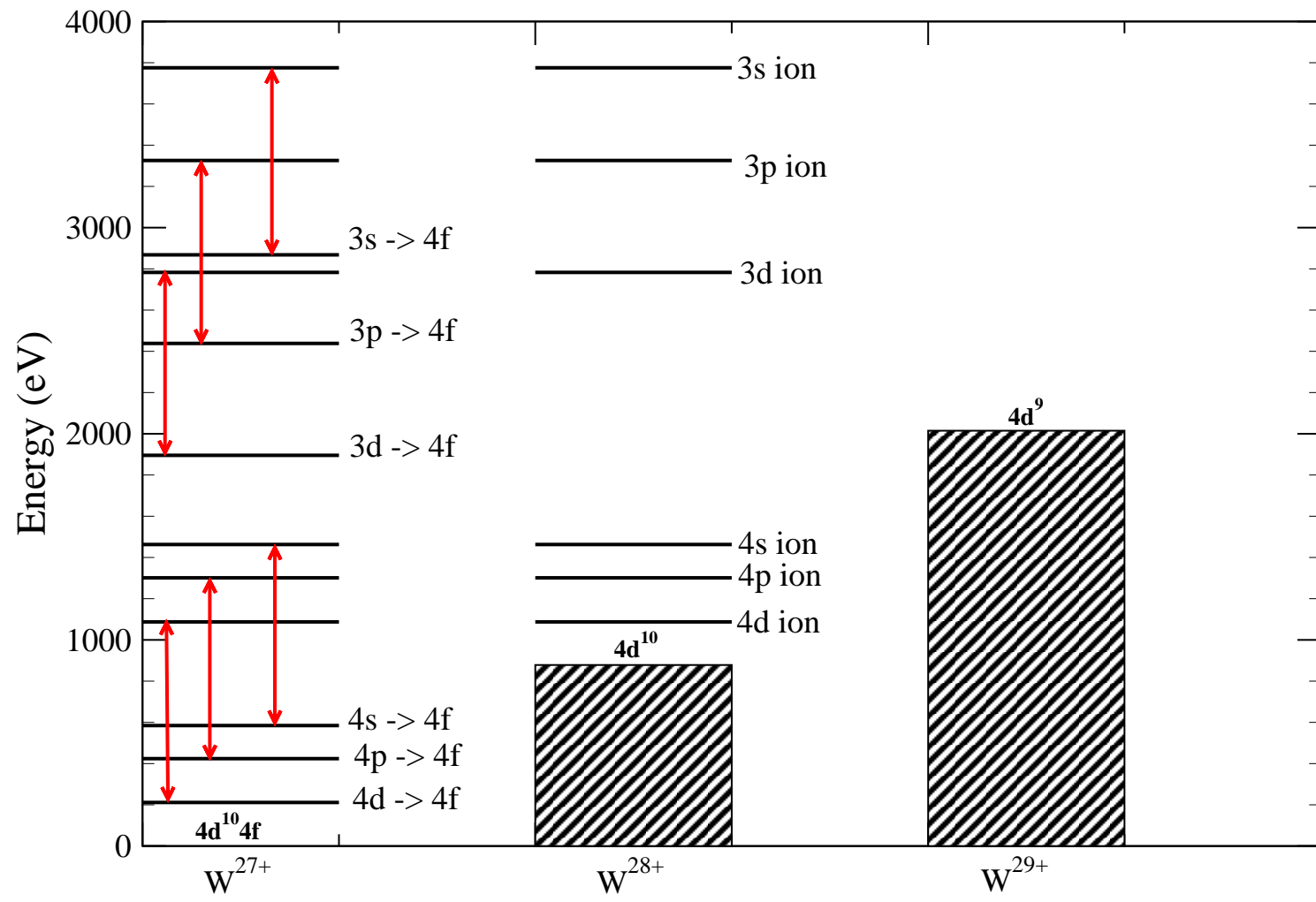
FIG. 1. Energy levels for W^{27+}

FIG. 2. Direct ionization cross sections for the outer subshells of W^{27+} . Solid line (red) : CADW ($4s + 4p + 4d + 4f$), dashed line (green) : CADW ($4p + 4d + 4f$), dot-dashed line (blue): CADW ($4d + 4f$), double dot-dashed line (violet): CADW ($4f$) ($1.0 \text{ Mb} = 1.0 \times 10^{-18} \text{ cm}^2$).

FIG. 3. Excitation-autoionization cross sections for the outer subshells of W^{27+} . Solid line (red) : CADW ($4d + 4p + 4s + 3d + 3p$), dashed line (green) : CADW including branching ratios, dot dashed line (red): SCADW ($4d + 4p + 4s$) [12], dot double dashed line (green): SCADW including branching ratios [12] ($1.0 \text{ Mb} = 1.0 \times 10^{-18} \text{ cm}^2$).

FIG. 4. Total single ionization cross section for W^{27+} . Solid line (red): CADW direct ionization plus excitation-autoionization including branching ratios, dashed line (green): CADW direct ionization only ($1.0 \text{ Mb} = 1.0 \times 10^{-18} \text{ cm}^2$).

Figure 1
09Jun2016



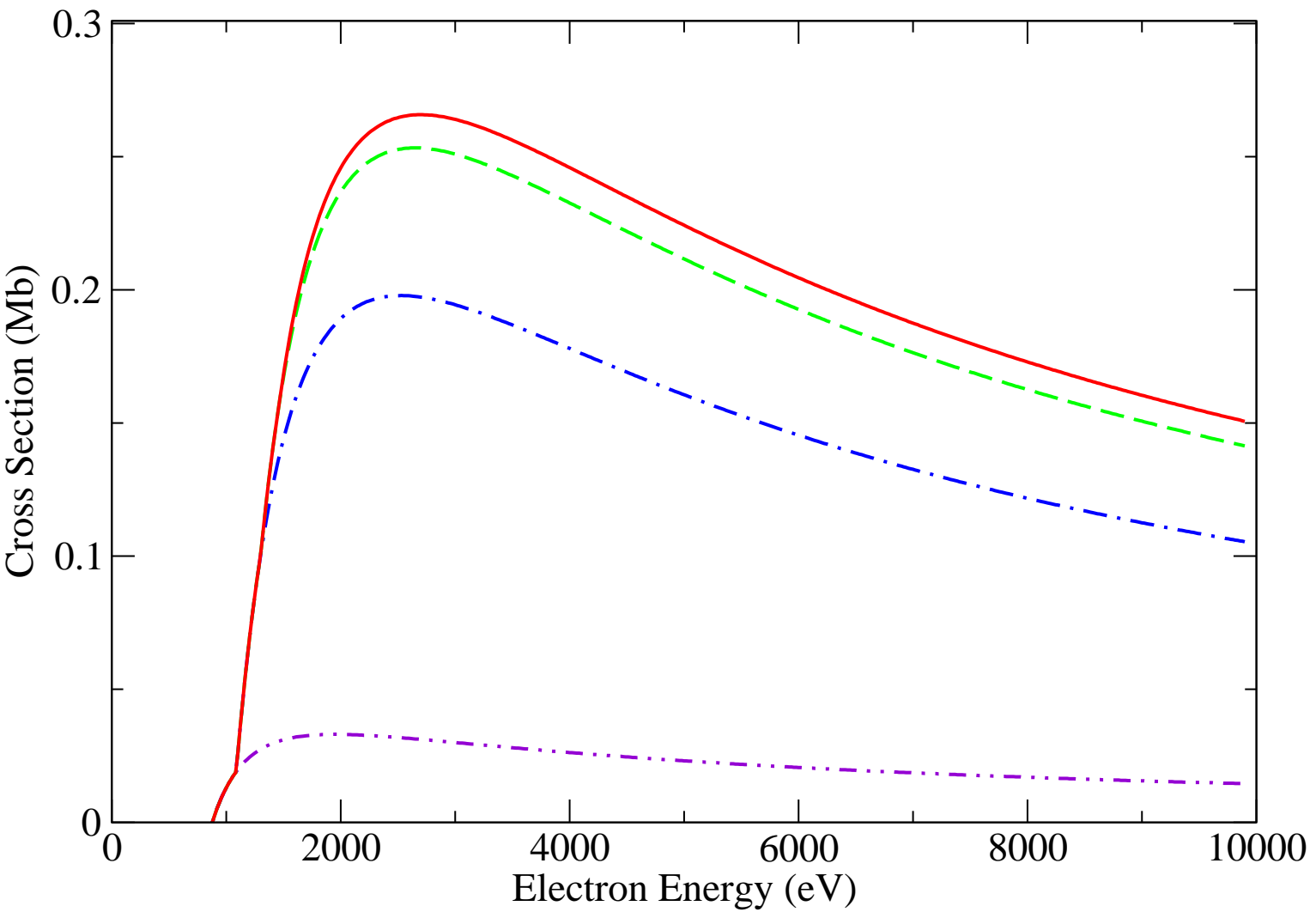


Figure 2

09Jun2016

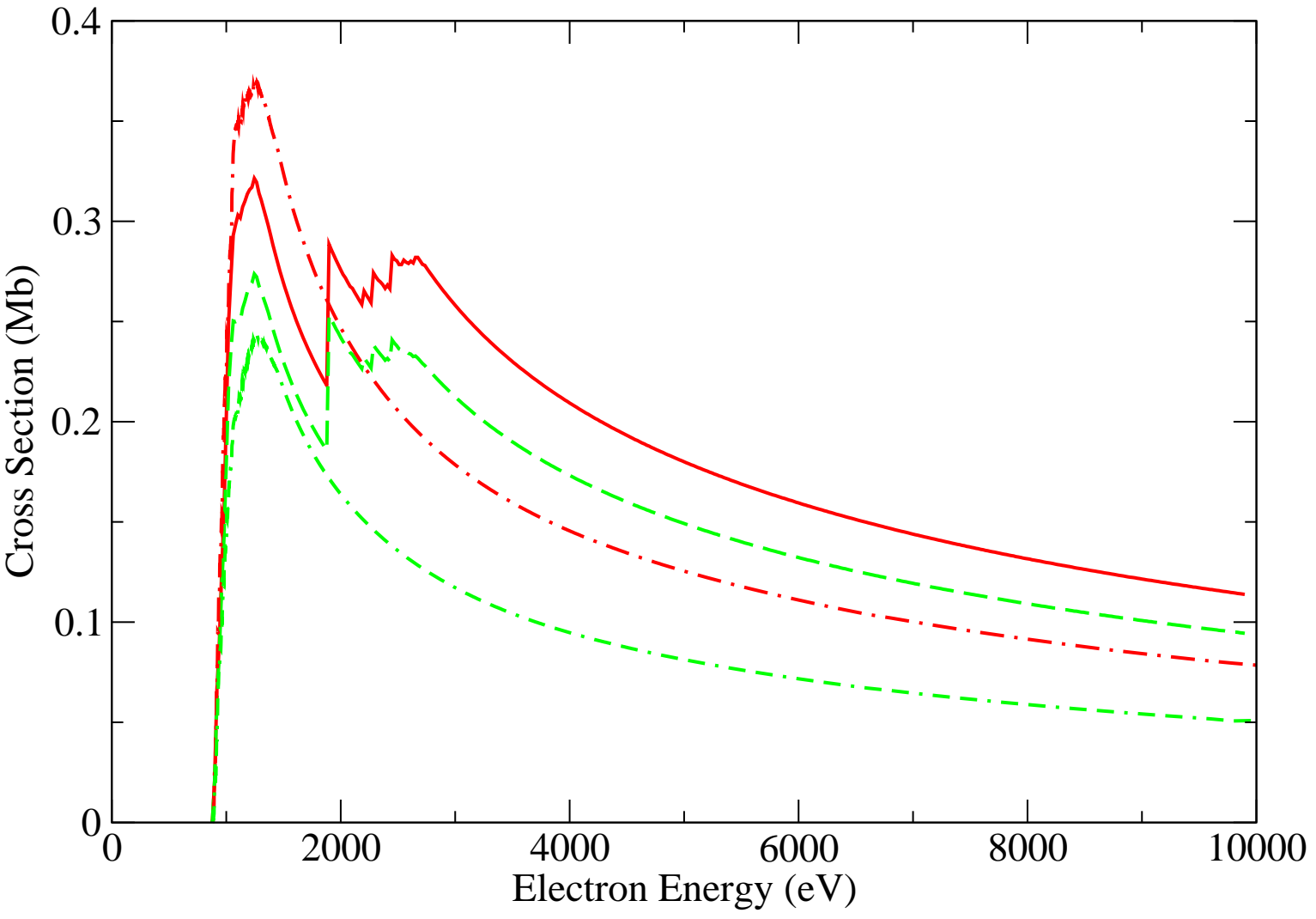


Figure 3

09Jun2016

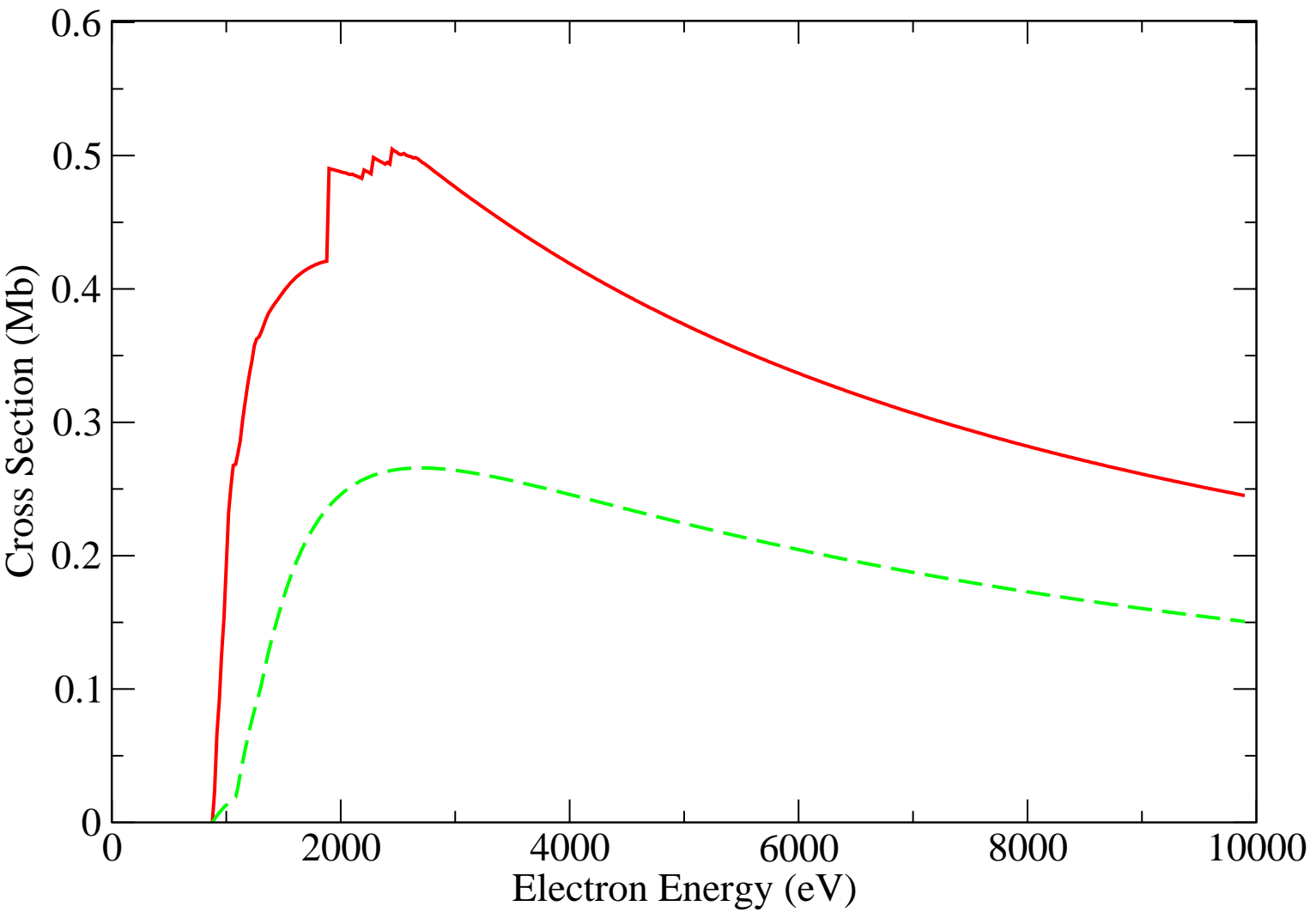


Figure 4

09Jun2016